*J. Am. Chem. Soc.* **1984**, *106*, 5164–5171

# Direct Preparation of a Siroheme Model Compound: Synthesis and Structure of (5,10,15,20-Tetramethylisobacteriochlorinato)nickel(II)

**Myunghyun Paik Suh,[1a] Paul N. Swepston,[1b] and James A. Ibers*[1b]**

*Contribution from the Department of Chemistry, Northwestern University, Evanston, Illinois 60201.* *Received January 16, 1984*

**Abstract:** The condensation reaction of pyrrole with acetaldehyde diethyl acetal in a glacial acetic acid solution of nickel acetate under an inert atmosphere yields (5,10,15,20-tetramethylisobacteriochlorinato)nickel(II), Ni(TMiBC), and 5,10,15,20-tetramethylporphyrinogen (TMporphyrinogen) as deduced by spectroscopy and for Ni(TMiBC) by X-ray analysis. Ni(TMiBC) crystallizes in the monoclinic space group $C_{2h}^5$-$P2_1/n$ ($a$ = 23.656 (2) Å, $b$ = 7.644 (1) Å, $c$ = 24.014 (2) Å, $\beta$ = 118.94 (1)°) with two independent molecules per asymmetric unit. The final agreement indices, based on 523 variables and 5307 unique reflections collected at −69 °C on an automatic diffractometer, are $R(F^2) = 0.086$ and $R_w(F^2) = 0.124$. The conventional $R$ index on $F$ for 4008 reflections having $F_o^2 > 3\sigma(F_o^2)$ is 0.065. The isobacteriochlorin macrocycle exhibits an $S_4$-ruffled conformation and a bond length pattern indicative of a reduction in aromaticity, both of which are more pronounced than those found in the corresponding porphyrin ((5,10,15,20-tetramethylporphyrinato)nickel(II), Ni(TMP)) and chlorin ((5,10,15,20-tetramethylchlorinato)nickel(II), Ni(TMC)) structures. This reduction in aromaticity is consistent with the $^1$H NMR spectra, which point to ring currents in the order Ni(TMiBC) < Ni(TMC) < Ni(TMP).

Studies on metalloporphyrins produce important information on the coordination sites in metallobiomolecules.[2] In certain biological systems, porphyrins that have been reduced, such as chlorins, bacteriochlorins, and isobacteriochlorins, occur as prosthetic groups.[3] An iron isobacteriochlorin, siroheme, is a common prosthetic group in assimilatory nitrite reductases as well as assimilatory and dissimilatory sulfite reductases, which catalyze the six-electron reduction of nitrite to ammonia and of sulfite to hydrogen sulfide, respectively.[4] The demetalated form of siroheme, sirohydrochlorin, has also been identified as an intermediate in the biosynthesis of vitamin $B_{12}$.[5-7] Thus, the study of isobacteriochlorins and their complexes has been the center of interest recently.[8-21]

**Table I.** Absorption Spectral Data for Ni(TMiBC) and Comparison with Ni(TMC), Ni(TMP), and Other Isobacteriochlorin Complexes

| complex[a] | solvent | $\lambda_{max}$, nm ($10^{-3}\epsilon$) |
|---|---|---|
| Ni(TMiBC) | benzene | 386 sh (23), 404 (37), 418 (42), 481 (4.3), 511 (3.0), 555 (5.3), 594 (16) |
| Ni(TMC)[b] | $CHCl_3$ | 421 (150), 510 (40), 583 (10), 618 (23) |
| Ni(TMP)[b] | $CHCl_3$ | 418 (190), 502 (30), 537 (12), 570 (25) |
| Zn(OEiBC)[c] | $CHCl_3$/MeOH | 368 (55), 386 (85), 400 (91), 490 (3.9), 524 (4.8), 553 (9.2), 597 (44), 642 (12) |
| Ni(OEiBC)[d] | $CH_2Cl_2$ | 365 sh (35.5), 386, (51.3), 518 (1.66), 548 (10.7), 593 (56.2) |
| Fe(OEiBC)[e] | $C_6H_6$ | 315 sh, 339 sh, 370 (31.7), 387 (33.6), 487 sh, 517 sh, 544 sh, 573 (10.3), 616 (21.1) |
| Zn(TPiBC)[f] | $CH_2Cl_2$ | no numbers are given[g] |

[a] OEiBC, octaethylisobacteriochlorin; TPiBC, tetraphenylisobacteriochlorin. [b] Reference 26. [c] Reference 10. [d] Reference 16. [e] Reference 11. [f] Reference 9. [g] The spectrum of Zn(TPiBC) is similar to that of Ni(TMiBC).

**Table II.** Chemical Shifts[a] of Protons in Ni(TMP), Ni(TMC), and Ni(TMiBC)

| compd | $\beta$-pyrrole | reduced ring | *meso*-methyl |
|---|---|---|---|
| Ni(TMP)[b] | 9.23 (s, 8 H) | | 4.11 (s, 12 H) |
| Ni(TMC)[b] | 8.65 (s, 2 H); 8.83, 8.46 (AX, 4 H) | 3.97 (s, 4 H) | 3.73 (s, 6 H),<br>3.08 (s, 6 H) |
| Ni(TMiBC)[c] | 8.14, 7.61 (AX, $J$ = 4.6, 4 H) | 3.45 (s, 8 H) | 3.29 (s, 3 H),<br>2.71 (s, 6 H),<br>2.27 (s, 3 H) |

[a] In parts per million downfield from $Me_4Si$; s, singlet; AX, AX system. [b] Reference 26. [c] Measured at $5 \times 10^{-3} - 5 \times 10^{-2}$ M in $CDCl_3$.

Most of the isobacteriochlorins and their complexes reported were prepared by reduction of the respective porphyrins,[10-12,22,23]

---

[1] (a) On leave from the Department of Chemistry Education, Seoul National University, Seoul 151, Korea. (b) Northwestern University.

[2] Ibers, J. A.; Holm, R. H. *Science* **1980**, *209*, 223–235.

[3] Porphyrins that contain two reducing equivalents (hydrogen atoms or alkyl groups) across the vicinal $C_b$ atoms of a single pyrrole ring are called chlorins. Porphyrins that contain two adjacent reduced pyrrole rings are called isobacteriochlorins while porphyrins that contain two non-adjacent reduced pyrrole rings are called bacteriochlorins. Porphyrins that are reduced at all four meso positions are called porphyrinogens.

[4] Murphy, M. J.; Siegel, L. M.; Kamin, H. *J. Biol. Chem.* **1973**, *248*, 2801–2814. Siegel, L. M.; Murphy, M. J.; Kamin, H. *Ibid.* **1973**, *248*, 251–264. Murphy, M. J.; Siegel, L. M.; Tove, S. R.; Kamin, H. *Proc. Natl. Acad. Sci. U.S.A.* **1974**, *71*, 612–616. Huckesby, D. P.; James, D. M.; Banwell, M. J.; Hewitt, E. J. *Phytochemistry* **1976**, *15*, 599–603. Vega, J. M.; Garrett, R. H. *J. Biol. Chem.* **1975**, *250*, 7980–7989. Vega, J. M.; Kamin, H. *Ibid.* **1977**, *252*, 896–909. Jacob, G. S.; Orme-Johnson, W. H. *Biochemistry*, **1979**, *18*, 2967–2980.

[5] Scott, A. I.; Irwin, A. J.; Siegel, L. M.; Shoolery, J. N. *J. Am. Chem. Soc.* **1978**, *100*, 316–318, 7987–7994.

[6] Bykovsky, V. Ya.; Zaitseva, N. I.; Umrihina, A. V.; Yavorskaya, A. N. *Priki. Biokhim. Mikrobiol.* **1976**, *12*, 825–833.

[7] Battersby, A. R.; Jones, K.; McDonald, E.; Robinson, J. A.; Morris, H. R. *Tetrahedron Lett.* **1977**, 2213–2216. Battersby, A. R.; McDonald, E.; Morris, H. R.; Thompson, M.; Williams, D. C.; Bykhovsky, V. Ya.; Zaitseva, N. I.; Bukin, V. N. *Ibid.* **1977**, 2217–2220. Battersby, A. R.; McDonald, E.; Thompson, M.; Bykhovsky, V. Ya. *J. Chem. Soc., Chem. Commun.* **1978**, 150–151.

[8] Richardson, P. F.; Chang, C. K.; Spaulding, L. D.; Fajer, J. *J. Am. Chem. Soc.* **1979**, *101*, 7736–7738. Chang, C. K.; Fajer, J. *Ibid.* **1980**, *102*, 848–851.

[9] Richardson, P. F.; Chang, C. K.; Hanson, L. K.; Spaulding, L. D.; Fajer, J. *J. Phys. Chem.* **1979**, *83*, 3420–3424.

[10] Stolzenberg, A. M.; Spreer, L. O.; Holm, R. H. *J. Chem. Soc., Chem. Commun.* **1979**, 1077–1078; *J. Am. Chem. Soc.* **1980**, *102*, 364–370.

[11] Stolzenberg, A. M.; Strauss, S. H.; Holm, R. H. *J. Am. Chem. Soc.* **1981**, *103*, 4763–4778.

[12] Barkigia, K. M.; Fajer, J.; Spaulding, L. D.; Williams, G. J. B. *J. Am. Chem. Soc.* **1981**, *103*, 176–181.

[13] Naab, P.; Lattman, R.; Angst, C.; Eschenmoser, A. *Angew. Chem., Int. Ed. Engl.* **1980**, *19*, 143–145.

[14] Montforts, P. F.; Otner, S.; Rassetty, V.; Eschenmoser, A.; Waggon, W. D.; Jones, K.; Battersby, A. R. *Angew. Chem., Int. Ed. Engl.* **1979**, *18*, 675–677.

[15] Chang, C. K. *Biochemistry* **1980**, *19*, 1971–1976.

[16] Johansen, J. E.; Angst, C.; Kratky, C.; Eschenmoser, A. *Angew. Chem., Int. Ed. Engl.* **1980**, *19*, 141–143.

[17] Angst, C.; Kajiwara, M.; Zass, E.; Eschenmoser, A. *Angew. Chem., Int. Ed. Engl.* **1980**, *19*, 140–141.

0002-7863/84/1506-5164$01.50/0

although a few isobacteriochlorins have been synthesized by stepwise ring-closure procedures[13,14] or by oxidation of the porphyrin followed by several elaborate procedures.[15] The preparations, however, usually involve difficulties in obtaining analytically and isomerically pure samples, and only a few X-ray structures have been reported for isobacteriochlorins or their complexes.[12,18-20]

In this paper we report the synthesis of a nickel(II) isobacteriochlorin complex, Ni(TMiBC),[24] and we compare its X-ray structures with those of its porphyrin (Ni(TMP))[25a-c] and chlorin (Ni(TMC))[25a,b] analogues. The complex was synthesized by the template condensation of pyrrole and acetaldehyde diethyl acetal (acetal) under anaerobic conditions. This appears to be the first isobacteriochlorin complex to be prepared directly from a condensation reaction.

## Experimental Section

**Reagents and Solvents.** All solvents were dried under Linde 4Å molecular sieves and distilled under nitrogen. Pyrrole and acetal were distilled and degassed prior to use.

**Physical Measurements.** All of the measurements were performed with the samples under an inert atmosphere. Electronic absorption spectra were recorded on a Perkin Elmer 330 spectrophotometer. Proton magnetic resonance spectra were measured on a JEOL FX-270 spectrometer. Chemical shifts are referenced to tetramethylsilane as an internal standard. Mass spectra were measured on a Hewlett Packard 5985A GC mass spectrometer.

**Preparation of Ni(TMiBC).** The preparative method is almost identical with that developed in this laboratory for Ni(TMP) and Ni(TMC)[26] except that all of the reagents were thoroughly degassed and the condensation reaction and the workup procedures were carried out with exclusion of air. In a typical preparation, $2 \times 10^{-2}$ mol of nickel acetate was dissolved in 400 mL of glacial acetic acid that contained 20 mL of acetic anhydride. Pyrrole ($8 \times 10^{-2}$ mol) and acetal ($8 \times 10^{-2}$ mol) dissolved in 25 mL of glacial acetic acid were added dropwise over a period of 30 min. The mixture was heated at 85–90 °C with stirring for 4 h and then filtered. The filtrate was diluted with 1000 mL of water and extracted with chloroform (4 × 100 mL). The chloroform layer was washed with water (2 × 150 mL) and then with 10% ammonia solution (3 × 150 mL). The washing was continued until the ammonia solution was not neutralized. The organic layer turned dark green. It was washed further with water (3 × 100 mL) and then dried over sodium sulfate. The solution was then concentrated under a reduced pressure to about 30 mL and chromatographed on a degassed dry alumina (neutral) column under oxygen-free nitrogen. The sample was eluted with a degassed mixture of 4:1 (v/v) toluene–chloroform. A small bright-green band containing Ni(TMC) was eluted first, followed by a dark bluish-green band containing Ni(TMiBC). The ratio of Ni(TMC)/Ni(TMiBC) depended on the amount of adventitious oxygen in the system. The purple eluate of Ni(TMiBC) was concentrated under a reduced pressure and left under nitrogen at room temperature. Several days later, Ni(TMiBC) precipitated from the solution, which was contaminated by 5–10% Ni(TMC) (as determined by $^1H$ NMR spectroscopy). Ni(TMiBC) was recrystallized from degassed chloroform. The yield was about 1% based on Ni. The UV/vis and $^1H$ NMR spectra are summarized in Tables I and II.

Table III. Crystallographic Details for Ni(TMiBC)

| | |
|---|---|
| formula | $C_{24}H_{24}N_4Ni$ |
| formula wt, amu | 427.20 |
| space group | $C_{2h}^5-P2_1/n$ |
| $a$, Å | 23.656 (2) |
| $b$, Å | 7.644 (1) |
| $c$, Å | 24.014 (2) |
| $\beta$, deg. | 118.94 (1) |
| vol, Å$^3$ | 3800 |
| $Z$ | 8 |
| density (calcd) (−69 °C), g/cm$^3$ | 1.486 |
| bounding planes[a] | {100}, 0.118; {$\bar{1}01$}, 0.146; {$\bar{1}02$}, 0.164; ($\bar{1}\bar{1}0$), (010) |
| crystal vol., mm$^3$ | 0.00715 |
| radiation | Cu K$\alpha$ ($\lambda(K\alpha_1)$ = 1.54056 Å, Ni filter) |
| linear abs. coeff., cm$^{-1}$ | 15.7 |
| transmission factors[b] | 0.676–0.852 |
| temp,[c] °C | −69 |
| detector aperture | 3.0 mm wide × 3.0 mm high; 32 cm from crystal |
| take-off angle, deg | 3.4 |
| scan speed | 2°/min in 2 $\theta$ |
| $2\theta$ limits | $3.5 \leq 2\theta \leq 122.5$ |
| background counts | 10 at each end of scan with rescan option[d] |
| scan range | 0.75 below K$\alpha_1$ to 0.75 above K$\alpha_2$ |
| data collected | $\pm h, +k, \pm l$ for $\lambda^{-1} \sin \theta \leq 0.2743$ Å$^{-1}$<br>$\pm h, +k, +l$ for $\lambda^{-1} \sin \theta \geq 0.2743$ Å$^{-1}$ |
| unique data | 5307 |
| unique data, with $F_o^2 > 3\sigma(F_o^2)$ | 4008 |
| final no. of variables | 523 |
| $R(F^2)$ | 0.086 |
| $R_w(F^2)$ | 0.124 |
| error in obsn of unit wt, e$^2$ | 1.76 |
| $R$ (on $F$ for $F_o^2 > 3\sigma(F_o^2)$) | 0.065 |

[a] The number following a form is the distance in mm between Friedel pairs. [b] An analytical absorption correction was applied. [c] The low-temperature system is based on a design by Huffman, J. C., Ph.D. Thesis, Indiana University, 1974. [d] The diffractometer was run under the Vanderbilt disk-oriented system (Lenhert, P. G. *J. Appl. Crystallogr.* **1975**, 8, 568–570).

**Isolation of TMporphyrinogen.** After the elution of Ni(TMiBC), a pale yellowish-green band was eluted which was identified as TMporphyrinogen. The solution was concentrated under a reduced pressure, and the product was crystallized by diffusing hexane into the solution. $^1H$ NMR (toluene-$d_8$): $\delta$ 1.33/1.35 (2 d, $J$ = 7.25, 4 $CH_3$), 3.95 (q, $J$ = 7.25, 4 CH), 5.87 (t, $J$ = 2.3, 8 pyrrole H), 6.98 (br, 4 NH). IR: 3430 cm$^{-1}$ (NH vs). MS: $m/e$ (principal peaks) 372 ($M^+$), 357, 186 ($M^{2+}$). The yield was about 0.2% based on Ni.

**X-ray Study of Ni(TMiBC).** Crystals of $C_{24}H_{24}N_4Ni$ were sealed in glass capillaries under an inert ($N_2$) atmosphere in order to carry out a preliminary photographic examination. Subsequent results showed that the crystals belong to the monoclinic system $C_{2h}^5-P2_1/n$ with two independent molecules in the asymmetric unit. An initial data set was collected at −150 °C with the use of Mo K$\alpha$ radiation. After the data were processed it was discovered that a significant number (~25%) of reflections of the type $h0l$ with $h + l$ odd (forbidden in $P2_1/n$) were weak but observable ($I > 3\sigma(I)$). The data crystal was remounted on the diffractometer and the $h0l$ reflections with $h + l$ odd were scanned as a function of temperature. Cu K$\alpha$ radiation was employed to eliminate the possibility of overlapping reflections. As the temperature was lowered, at approximately −97 °C some of the $h0l$ with $h + l$ odd reflections became observable. The transition was not sharp but it was reversible; the net intensities of the observable $h0l$ with $h + l$ odd reflections increased steadily (at a faster rate than the general reflections) as the temperature was lowered to −150 °C and disappeared if the crystal was warmed up above −97 °C. A new data set was collected with Cu K$\alpha$ radiation on a Picker FACS-1 diffractometer at a temperature of −69 °C. Accurate unit cell parameters were determined by least-squares refinement of 19 high-angle reflections that had been automatically centered. Six standard reflections measured at 100 reflection intervals showed no indication of crystal decay during the course of data collection.

---

(18) Kratky, C.; Angst, C.; Johansen, J. E. *Angew. Chem., Int. Ed. Engl.* **1981**, *20*, 211–212.

(19) Cruse, W. B. T.; Harrison, P. J.; Kennard, O. *J. Am. Chem. Soc.* **1982**, *104*, 2376–2380.

(20) Barkigia, K. M.; Fajer, J.; Chang, C. K.; Williams, G. J. B. *J. Am. Chem. Soc.* **1982**, *104*, 315–317.

(21) Johansen, J. E.; Piermattie, V.; Angst, C.; Diener, E.; Kratky, C.; Eschenmoser, A. *Angew. Chem., Int. Ed. Engl.* **1981**, *20*, 261–263.

(22) Whitlock, H. W.; Hanover, R., Jr.; Oester, M. Y.; Bower, B. K. *J. Am. Chem. Soc.* **1969**, *91*, 7485–7489.

(23) (a) Harel, Y.; Manassen, J. *J. Am. Chem. Soc.* **1978**, *100*, 6228–6234. (b) Scheer, H.; Katz, J. J. "Porphyrins and Metalloporphyrins"; Smith, K. M., Ed., Elsevier: Amsterdam, 1964; pp 399–514.

(24) Abbreviations: TMiBC, 5,10,15,20-tetramethylisobacteriochlorinato; TMP, 5,10,15,20-tetramethylporphyrinato; TMC, 5,10,15,20-tetramethylchlorinato; OEP, 2,3,7,8,12,13,17,18-octaethylporphyrinato; OEC, 2,3,7,8,12,13,17,18-octaethylchlorinato; OEiBC, 2,3,7,8,12,13,17,18-octaethylisobacteriochlorinato; TMporphyrinogen, 5,10,15,20-tetramethylporphyrinogen; TPiBC, 5,10,15,20-tetraphenylisobacteriochlorinato; OMiBC, 2,2,8,8,12,13,17,18-octamethylisobacteriochlorinato; TPP, 5,10,15,20-tetraphenylporphyrinato.

(25) (a) Ulman, A.; Gallucci, J.; Fisher, D.; Ibers, J. A. *J. Am. Chem. Soc.* **1980**, *102*, 6852–6854. (b) Gallucci, J.; Swepston, P. N.; Ibers, J. A. *Acta Crystallogr., Sect. B* **1982**, *B38*, 2134–2139. (c) Kutzler, F. W.; Swepston, P. N.; Berkovitch-Yellin, Z.; Ellis, D. E.; Ibers, J. A. *J. Am. Chem. Soc.* **1983**, *105*, 2996–3004.

(26) Ulman, A.; Fisher, D.; Ibers, J. A. *J. Heterocycl. Chem.* **1982**, *19*, 409–413.

**Table IV.** Positional Parameters for the Non-Hydrogen Atoms of Ni(TMiBC)

| atom | *x* | *y* | *z* | atom | *x* | *y* | *z* |
|---|---|---|---|---|---|---|---|
| Ni | 0.252885 (29) | 0.059939 (88) | 0.807376 (28) | C24 | 0.46602 (21) | 0.23887 (65) | 0.97047 (22) |
| Ni | 0.195592 (30) | −0.578463 (89) | 0.171052 (30) | N1′ | 0.19036 (16) | −0.54763 (45) | 0.24839 (15) |
| N(1) | 0.33468 (15) | 0.08692 (43) | 0.80913 (15) | N2′ | 0.28759 (16) | −0.54781 (44) | 0.21899 (17) |
| N(2) | 0.20850 (15) | 0.07383 (42) | 0.71616 (14) | N3′ | 0.20070 (16) | −0.61015 (44) | 0.09416 (16) |
| N(3) | 0.17146 (15) | 0.03068 (44) | 0.80571 (15) | N4′ | 0.10387 (15) | −0.60893 (43) | 0.12365 (15) |
| N(4) | 0.29668 (15) | 0.04872 (44) | 0.89808 (15) | C1′ | 0.13415 (24) | −0.49556 (60) | 0.25110 (22) |
| C(1) | 0.39156 (18) | 0.14672 (56) | 0.86012 (21) | C2′ | 0.15203 (28) | −0.45983 (69) | 0.31924 (24) |
| C(2) | 0.44181 (19) | 0.17439 (65) | 0.83880 (23) | C3′ | 0.21699 (27) | −0.54137 (68) | 0.35710 (22) |
| C(3) | 0.41368 (21) | 0.08772 (66) | 0.77591 (24) | C4′ | 0.23871 (24) | −0.56999 (58) | 0.30759 (20) |
| C(4) | 0.34472 (20) | 0.05429 (55) | 0.75869 (20) | C5′ | 0.30206 (24) | −0.60142 (64) | 0.32592 (21) |
| C(5) | 0.29960 (22) | 0.01124 (57) | 0.69851 (20) | C6′ | 0.32434 (21) | −0.56938 (57) | 0.28263 (22) |
| C(6) | 0.23524 (21) | 0.03984 (55) | 0.67730 (18) | C7′ | 0.39408 (23) | −0.53864 (75) | 0.30415 (27) |
| C(7) | 0.18693 (22) | 0.05465 (60) | 0.60898 (19) | C8′ | 0.39383 (23) | −0.45655 (69) | 0.24816 (30) |
| C(8) | 0.13006 (21) | 0.14641 (61) | 0.60987 (19) | C9′ | 0.32831 (21) | −0.49515 (62) | 0.19428 (25) |
| C(9) | 0.14488 (19) | 0.12036 (53) | 0.67730 (18) | C10′ | 0.31158 (23) | −0.49926 (62) | 0.13259 (27) |
| C(10) | 0.09903 (19) | 0.13105 (57) | 0.69686 (20) | C11′ | 0.25260 (23) | −0.56836 (60) | 0.08536 (23) |
| C(11) | 0.11302 (19) | 0.07124 (56) | 0.75775 (20) | C12′ | 0.23900 (27) | −0.61956 (72) | 0.02425 (24) |
| C(12) | 0.06399 (20) | 0.02818 (65) | 0.77446 (22) | C13′ | 0.18031 (27) | −0.69483 (67) | −0.00501 (22) |
| C(13) | 0.09382 (21) | −0.04222 (66) | 0.83230 (22) | C14′ | 0.15519 (22) | −0.68751 (58) | 0.03822 (19) |
| C(14) | 0.16172 (20) | −0.03934 (56) | 0.85471 (19) | C15′ | 0.09320 (21) | −0.73224 (59) | 0.02390 (18) |
| C(15) | 0.20949 (22) | −0.07141 (56) | 0.91526 (20) | C16′ | 0.06823 (19) | −0.68637 (56) | 0.06425 (19) |
| C(16) | 0.27305 (21) | −0.02330 (57) | 0.93714 (19) | C17′ | 0.00222 (21) | −0.69276 (66) | 0.04738 (22) |
| C(17) | 0.32152 (24) | −0.01174 (66) | 1.00032 (20) | C18′ | −0.00258 (20) | −0.61407 (66) | 0.09532 (24) |
| C(18) | 0.37381 (23) | 0.06829 (65) | 1.00317 (20) | C19′ | 0.05907 (19) | −0.56526 (57) | 0.14224 (21) |
| C(19) | 0.35824 (20) | 0.10027 (58) | 0.93927 (18) | C20′ | 0.07512 (22) | −0.49723 (59) | 0.20297 (22) |
| C(20) | 0.40339 (19) | 0.16456 (59) | 0.92035 (20) | C21′ | 0.34926 (26) | −0.64699 (72) | 0.39294 (23) |
| C(21) | 0.32033 (23) | −0.04209 (63) | 0.64971 (22) | C22′ | 0.36136 (26) | −0.44416 (74) | 0.11188 (30) |
| C(22) | 0.03166 (21) | 0.18288 (69) | 0.64890 (22) | C23′ | 0.04958 (24) | −0.82098 (66) | −0.03783 (21) |
| C(23) | 0.19191 (24) | −0.15449 (66) | 0.96255 (21) | C24′ | 0.01884 (25) | −0.43951 (75) | 0.21240 (27) |

Experimental details are given in Table III.

All calculations were performed on a Harris 800 computer with programs standard in this laboratory. Conventional atomic scattering factors were used for the non-hydrogen[27] and hydrogen[28] atoms. Anomalous dispersion corrections[29] were applied to nickel atoms; values of $\Delta f'$ and $\Delta f''$ were those of Cromer and Waber.[27]

The positions of the two independent nickel atoms were obtained from an *E* map with phases calculated by the program MULTAN80.[30] Although additional atomic positions were located in the *E* map, the incompleteness and geometric distortions of the model led us to retain only the nickel atom positions and to extend the model with the direct methods program DIRDIF.[31] Experience in this laboratory has shown this method to be more efficient in obtaining a complete undistorted model than standard Fourier and least-squares-refinement techniques.

The measured intensities were corrected for absorption, and the redundant data were averaged. The model was initially refined on $F_o$ ($F_o^2 > 3\sigma(F_o^2)$) in a block-diagonal fashion with the variables of each independent molecule defining a separate matrix. All non-hydrogen atoms were refined anisotropically. Hydrogen atoms were added as fixed contributions to the structure factors. Idealized methyl-hydrogen positions (C–H = 0.95 Å; H–C–H = 109.5°) were obtained from a least-squares adjustment of their observed positions, and the remaining hydrogen positions were calculated by assuming idealized geometries. Each hydrogen atom was assigned an isotropic thermal parameter 1 Å$^2$ greater than the equivalent isotropic thermal parameter of the atom to which it is attached. In the final stages of model adjustment, full-matrix least-squares refinement on $F_o^2$ (using all unique intensities) was employed. The final agreement indices are listed in Table III. The largest peak in the final difference electron density map (0.63 (9) e/Å$^3$) is near one of the nickel atoms and has the same peak height as was found for a typical hydrogen atom.

The positional parameters for the non-hydrogen atoms are listed in Table IV. Table V presents the anisotropic thermal parameters,[32] Table VI presents the hydrogen atom parameters,[32] and Table VII contains the final values of $10|F_o|$ and $10|F_c|$.[32] A negative entry in Table VII implies that $F_o^2$ was observed to be negative.

**Scheme I**

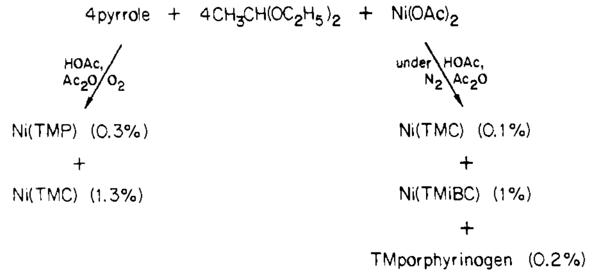

**Scheme II**

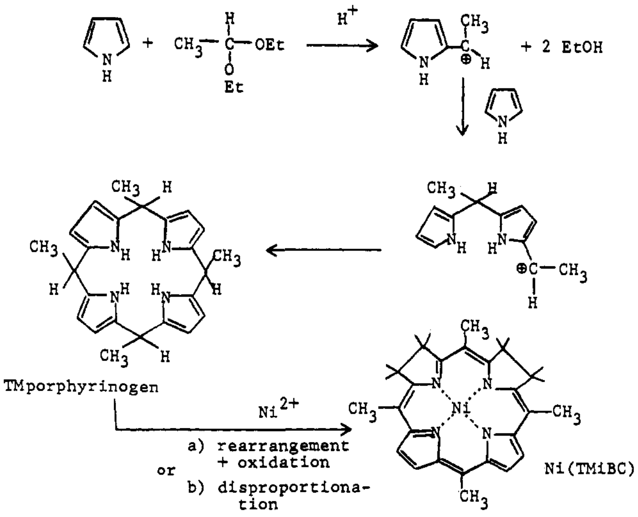

## Results and Discussion

Previous work in this laboratory showed that the condensation reaction of pyrrole and acetal in the presence of Ni(II) yields Ni(TMC) and Ni(TMP) (4:1 ratio, total yield 1.6%) when the

---

(27) Cromer, D. T.; Waber, J. T. "International Tables for X-ray Crystallography"; Kynoch Press: Birmingham, England, 1974; Vol. IV, p 71.

(28) Stewart, R. F.; Davidson, E. R.; Simpson, W. T. *J. Chem. Phys.* **1965**, *42*, 3175–3187.

(29) Ibers, J. A.; Hamilton, W. C. *Acta Crystallogr.* **1964**, *17*, 781–782.

(30) The 1980 version of the direct methods program MULTAN. Germain, G.; Main, P.; Woolfson, M. M. *Acta Crystallogr., Sect. A* **1971**, *A27*, 368–376.

(31) DIRDIF: Direct methods applied to Difference structure factors to strengthen Fourier methods. Beurskens, P. T.; Bosman, W. P.; Doesburg, H. M.; Gould, R. O.; van den Hark, Th. E. M.; Prick, P. A. J. "Computational Crystallography"; Sayre, D., Ed.; Clarendon Press: Oxford, 1982; p 516.

(32) Supplementary material.

**Table VIII.** Bond Lengths (Å) for the Non-Hydrogen Atoms of Ni(TMiBC)

| distance | molecule 1 | molecule 2 | distance | molecule 1 | molecule 2 |
|---|---|---|---|---|---|
| Ni-N(1) | 1.926 (3) | 1.934 (3) | C(7)-C(8) | 1.527 (6) | 1.481 (8) |
| Ni-N(2) | 1.920 (3) | 1.922 (3) | C(8)-C(9) | 1.495 (5) | 1.491 (6) |
| Ni-N(3) | 1.920 (3) | 1.923 (3) | C(9)-C(10) | 1.377 (6) | 1.336 (6) |
| Ni-N(4) | 1.908 (3) | 1.915 (3) | C(10)-C(11) | 1.410 (6) | 1.407 (6) |
| N(1)-C(1) | 1.387 (5) | 1.419 (5) | C(11)-C(12) | 1.437 (6) | 1.398 (6) |
| N(1)-C(4) | 1.366 (5) | 1.336 (5) | C(12)-C(13) | 1.330 (6) | 1.345 (7) |
| N(2)-C(6) | 1.382 (5) | 1.354 (5) | C(13)-C(14) | 1.426 (6) | 1.425 (6) |
| N(2)-C(9) | 1.380 (5) | 1.412 (6) | C(14)-C(15) | 1.364 (5) | 1.378 (6) |
| N(3)-C(11) | 1.339 (5) | 1.380 (5) | C(15)-C(16) | 1.381 (6) | 1.402 (6) |
| N(3)-C(14) | 1.410 (5) | 1.383 (5) | C(16)-C(17) | 1.393 (5) | 1.411 (6) |
| N(4)-C(16) | 1.415 (5) | 1.390 (5) | C(17)-C(18) | 1.352 (7) | 1.351 (7) |
| N(4)-C(19) | 1.364 (5) | 1.375 (5) | C(18)-C(19) | 1.415 (6) | 1.395 (6) |
| C(1)-C(2) | 1.519 (6) | 1.504 (6) | C(19)-C(20) | 1.435 (6) | 1.416 (6) |
| C(2)-C(3) | 1.480 (6) | 1.491 (7) | C(20)-C(1) | 1.341 (6) | 1.313 (6) |
| C(3)-C(4) | 1.498 (5) | 1.522 (6) | C(5)-C(21) | 1.528 (5) | 1.490 (6) |
| C(4)-C(5) | 1.358 (6) | 1.363 (6) | C(10)-C(22) | 1.499 (5) | 1.542 (6) |
| C(5)-C(6) | 1.369 (6) | 1.396 (7) | C(15)-C(23) | 1.524 (6) | 1.497 (6) |
| C(6)-C(7) | 1.482 (5) | 1.490 (6) | C(20)-C(24) | 1.497 (5) | 1.520 (6) |

reaction is carried out in the presence of air.[25a,26] The same reaction performed under an inert atmosphere in the present study, however, produces Ni(TMiBC) and some TMporphyrinogen, Scheme I. Such direct preparation of an isobacteriochlorin derivative from the condensation of pyrrole and aldehyde apparently has not been reported previously. The ratio of Ni(TMC)/Ni(TMiBC) increases as oxygen is introduced into the system; if sufficient oxygen is introduced Ni(TMP) is produced as well, fully consistent with the previous work.[26] Oxidation of isobacteriochlorin complexes to chlorin complexes is known to proceed via cationic radicals and dications.[10,11,33-35] Nevertheless, solutions of Ni(TMiBC) are surprisingly stable; a $5 \times 10^{-5}$ M toluene solution on standing in the air in the dark over a 10-day period at room temperature yielded a Ni(TMC)/Ni(TMiBC) ratio of 1/3.

We propose that Scheme II is a plausible route for the formation of Ni(TMiBC). The isolation of TMporphyrinogen in the present study is significant, since porphyrinogens are known to lead to isobacteriochlorins.[16,21] In addition, it is known that acids catalyze the cyclization step and that the addition of an anhydride also enhances the yield of the cyclization product by suppressing the polymerization of the cationic intermediates.[36] The formation of Ni(TMiBC) from the porphyrinogen, the product of the cyclization step, may arise from insertion of Ni followed by either oxidation or disproportionation. Such processes have been observed for the formation of Ni(OEiBC) from the free octaethyl porphyrinogen.[16,21] The present result that the chlorin complex is formed without the formation of the corresponding porphyrin complex stands in marked contrast with Dolphin's suggestion that chlorins are produced by the reduction of pre-formed porphyrins.[37]

The electronic spectrum of Ni(TMiBC) in benzene is shown in Figure 1 and summarized in Table I. The spectral results obtained from other related systems are also tabulated. Comparison of the spectra reveals the presence in Ni(TMiBC) of the characteristic chromophore of isobacteriochlorinato metal complexes. Extinction coefficients of the Soret and visible bands of Ni(TMiBC) are smaller than those of Ni(TMC) or Ni(TMP), and the ratio of the intensities of the Soret band to the strongest visible band is also smaller for Ni(TMiBC) than for Ni(TMC) or Ni(TMP). Similar observations also have beem made for $Fe^{II,III}$OEP, -OEC, and -OEiBC complexes.[11,24]

The $^1H$ NMR spectrum of Ni(TMiBC) is compared with those of Ni(TMC) and Ni(TMP) in Table II. The reduced ring protons, the *meso*-alkyl protons, as well as the $\beta$-pyrrole protons are gradually shifted to higher field on going from Ni(TMP) to Ni(TMiBC). This indicates[23] that the ring currents are in the order of Ni(TMP) > Ni(TMC) > Ni(TMiBC) and, consequently, Ni(TMiBC) has the lowest degree of aromaticity.

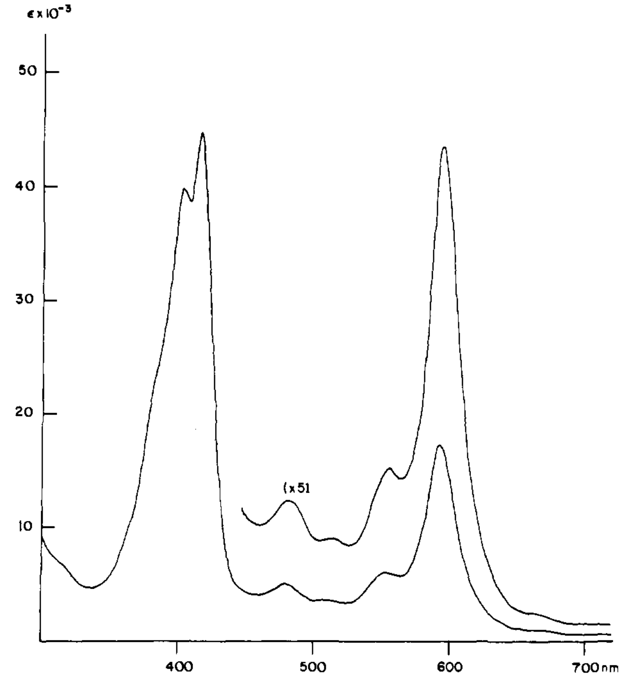

**Figure 1.** UV–vis absorption spectrum of Ni(TMiBC) in benzene.

Structural characterization of Ni(TMiBC) by X-ray crystallography was undertaken in order to ascertain how the reduction of the porphyrin-conjugated $\pi$-electron system is manifested in the bonding pattern and general conformation of the isobacteriochlorin macrocycle. Although several free base[18-20] and metallo-[12,20] isobacteriochlorins have been characterized by X-ray diffraction, Ni(TMiBC) is unique in that the structures of the porphyrin (Ni(TMP)) and chlorin (Ni(TMC)) analogues with exactly the same metal and ring substituents are already known.[25] Thus the structure of Ni(TMiBC) provides us with an opportunity to assess the metrical changes that occur as a porphyrin ring is progressively reduced.[38]

Ni(TMiBC) crystallizes with two independent molecules in the unit cell: one such molecule is illustrated in Figure 2 along with the atom- and ring-numbering schemes. For ease of comparison,

---

(33) Richardson, P. F.; Chang, C. K.; Spaulding, L. D.; Fajer, J. *J. Am. Chem. Soc.* **1979**, *101*, 7736–7738; *J. Phys. Chem.* **1979**, *83*, 3420–3424.

(34) Chang, C. K.; Fajer, J. *J. Am. Chem. Soc.* **1980**, *102*, 848–851.

(35) Chang, C. K.; Hanson, L. K.; Richardson, P. F.; Young, R.; Fajer, J. *Proc. Natl. Acad. Sci. U.S.A.* **1981**, *78*, 2652–2656.

(36) Alder, A. D.; Sklar, L.; Longo, F. R.; Finarelli, J. D.; Finarelli, M. G. *J. Heterocycl. Chem.* **1968**, *5*, 669–678.

(37) Dolphin, D. *J. Heterocycl. Chem.* **1970**, *7*, 275–283.

(38) Of course, since the three crystal structures are different, some differences in molecular structure could be ascribed to crystal-packing differences among Ni(TMP), Ni(TMC), and Ni(TM*i*BC).

**Table IX.** Bond Angles (deg) for the Non-Hydrogen Atoms of Ni(TMiBC)

| bond angle | molecule 1 | molecule 2 |
|---|---|---|
| N(1)–Ni–N(2) | 90.5 (1) | 89.4 (1) |
| N(1)–Ni–N(3) | 179.5 (1) | 179.8 (1) |
| N(1)–Ni–N(4) | 89.7 (1) | 90.3 (1) |
| N(2)–Ni–N(3) | 89.6 (1) | 90.6 (1) |
| N(2)–Ni–N(4) | 179.4 (1) | 179.7 (1) |
| N(3)–Ni–N(4) | 90.2 (1) | 89.6 (1) |
| Ni–N(1)–C(1) | 126.2 (3) | 125.1 (3) |
| Ni–N(1)–C(4) | 124.4 (3) | 125.9 (3) |
| Ni–N(2)–C(6) | 125.7 (3) | 125.7 (3) |
| Ni–N(2)–C(9) | 127.0 (3) | 126.0 (3) |
| Ni–N(3)–C(11) | 126.8 (3) | 126.3 (3) |
| Ni–N(3)–C(14) | 126.5 (3) | 127.2 (3) |
| Ni–N(4)–C(16) | 126.1 (3) | 127.7 (3) |
| Ni–N(4)–C(19) | 127.9 (3) | 127.4 (3) |
| N(1)–C(1)–C(2) | 109.4 (4) | 108.9 (4) |
| N(1)–C(4)–C(3) | 110.9 (4) | 112.0 (4) |
| N(2)–C(6)–C(7) | 111.9 (4) | 111.8 (5) |
| N(2)–C(9)–C(8) | 112.0 (4) | 109.0 (4) |
| N(3)–C(11)–C(12) | 110.1 (4) | 109.0 (4) |
| N(3)–C(14)–C(13) | 107.5 (4) | 108.7 (4) |
| N(4)–C(16)–C(17) | 108.4 (4) | 110.3 (4) |
| N(4)–C(19)–C(18) | 110.3 (4) | 110.0 (4) |
| C(1)–N(1)–C(4) | 109.4 (4) | 109.0 (4) |
| C(6)–N(2)–C(9) | 107.3 (3) | 108.2 (4) |
| C(11)–N(3)–C(14) | 106.7 (3) | 106.4 (4) |
| C(16)–N(4)–C(19) | 104.9 (3) | 104.9 (3) |
| C(1)–C(2)–C(3) | 104.1 (4) | 104.6 (4) |
| C(4)–C(3)–C(2) | 104.5 (4) | 102.8 (4) |
| C(6)–C(7)–C(8) | 103.4 (4) | 103.6 (4) |
| C(9)–C(8)–C(7) | 102.0 (3) | 104.5 (4) |
| C(11)–C(12)–C(13) | 107.0 (4) | 108.9 (4) |
| C(14)–C(13)–C(12) | 108.6 (4) | 107.0 (4) |
| C(16)–C(17)–C(18) | 109.6 (4) | 106.1 (4) |
| C(19)–C(18)–C(17) | 105.8 (4) | 108.7 (4) |
| N(1)–C(1)–C(20) | 126.3 (4) | 125.3 (4) |
| N(1)–C(4)–C(5) | 127.2 (4) | 127.4 (5) |
| N(2)–C(6)–C(5) | 124.7 (4) | 126.5 (4) |
| N(2)–C(9)–C(10) | 124.5 (4) | 124.3 (4) |
| N(3)–C(11)–C(10) | 126.4 (4) | 124.9 (4) |
| N(3)–C(14)–C(15) | 124.9 (4) | 125.6 (4) |
| N(4)–C(16)–C(15) | 123.9 (4) | 124.5 (4) |
| N(4)–C(19)–C(20) | 124.5 (4) | 124.0 (4) |
| C(4)–C(5)–C(6) | 121.1 (4) | 118.7 (4) |
| C(9)–C(10)–C(11) | 120.4 (4) | 123.3 (5) |
| C(14)–C(15)–C(16) | 123.1 (4) | 121.3 (4) |
| C(19)–C(20)–C(1) | 120.5 (4) | 123.4 (4) |
| C(5)–C(4)–C(3) | 121.7 (4) | 120.5 (4) |
| C(5)–C(6)–C(7) | 123.2 (4) | 121.6 (4) |
| C(10)–C(9)–C(8) | 123.4 (4) | 126.4 (5) |
| C(10)–C(11)–C(12) | 123.2 (4) | 125.9 (5) |
| C(15)–C(14)–C(13) | 126.9 (4) | 125.3 (4) |
| C(15)–C(16)–C(17) | 127.0 (4) | 124.8 (4) |
| C(20)–C(1)–C(2) | 124.1 (4) | 125.4 (5) |
| C(20)–C(19)–C(18) | 124.0 (4) | 125.8 (4) |
| C(4)–C(5)–C(21) | 120.1 (4) | 121.5 (5) |
| C(6)–C(5)–C(21) | 118.0 (4) | 119.3 (5) |
| C(9)–C(10)–C(22) | 118.3 (4) | 119.2 (5) |
| C(11)–C(10)–C(22) | 120.7 (4) | 117.2 (5) |
| C(14)–C(15)–C(23) | 119.0 (4) | 120.0 (4) |
| C(16)–C(15)–C(23) | 117.8 (4) | 118.6 (4) |
| C(1)–C(20)–C(24) | 121.0 (4) | 120.1 (5) |
| C(19)–C(20)–C(24) | 118.3 (4) | 116.3 (4) |

bond lengths and atomic deviations from the plane of the macrocycle are displayed for both molecules in Figure 3. Tabulated bond distances and angles are available as Tables VIII and IX.

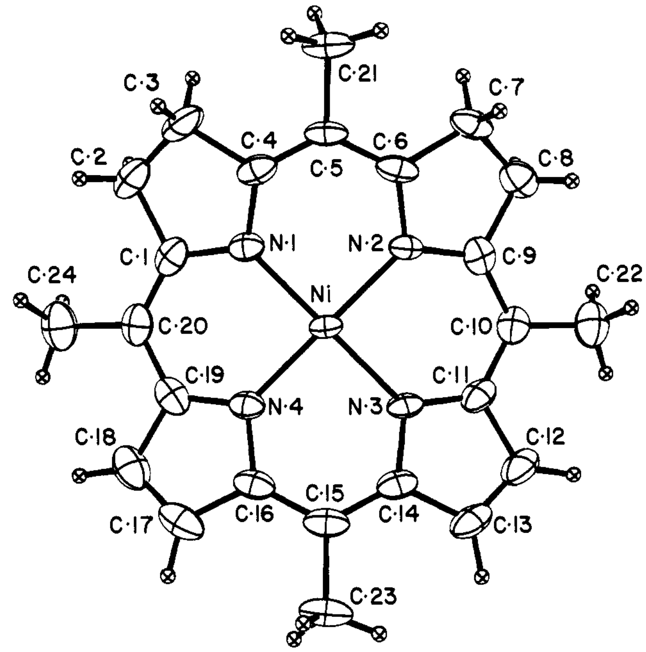

**Figure 2.** Drawing of Ni(TMiBC) molecule 1 (50% probability thermal ellipsoids) along with the atom- and ring-numbering schemes.

Of immediate interest is the metrical distinguishability of the reduced pyrrole rings (hereafter referred to as pyrroline rings) from the pyrrole rings. Lengthening of the $C_b$–$C_b$[39] bonds owing to reduction in bond order should be a sensitive criterion for these systems, although this is not always the case.[40] Pyrroline $C_b$–$C_b$ bond distances in chlorins[24,25,41,42] and isobacteriochlorins[12,18-20] have a wide range of values (1.416 (5)–1.533 (7) Å), the low end of which (1.416 (5) Å, Zn(TPiBC)(py)[12]) is only slightly longer than the usual $C_b$–$C_b$ bond length for a pyrrole ring (~1.36 Å[12]). On the other hand, the value of 1.533 (7) Å found in $H_2$(OMiBC)[19] is equal to the value of a typical C–C single bond (~1.54 Å). For Ni(TMiBC) the $C_b$–$C_b$ pyrroline bond lengths (range 1.480 (6)–1.527 (6) Å; mean 1.495 (9) Å) are easily distinguished from the $C_b$–$C_b$ pyrrole bond lengths (range 1.330 (6)–1.352 (7) Å; mean 1.344 (9) Å). Other geometrical parameters, such as the $C_a$–$C_b$ bond lengths (pyrroline mean value 1.50 (1) Å; pyrrole mean value 1.41 (1) Å), the $C_a$–N–$C_a$ bond angles (pyrroline mean value 108.5 (8)°; pyrrole mean value 105.7 (8)°), and the $C_a$–$C_b$–$C_b$–$C_a$ torsion angles (pyrroline mean value 15 (2)°; pyrrole mean value 2.5 (5)°), can also be used to differentiate between the pyrroline and pyrrole rings.

Relative to Ni(TMP), the bond length pattern of Ni(TMC) was found to have a long–short alternation that was a clear indication of reduction in $\pi$ delocalization.[25a,b] Because Ni(TMiBC) has an additional pyrroline ring, the structure was expected to reflect an even greater disruption in the $\pi$-delocalized system. This is indeed the case and is most clearly evident when a comparison is made between the $C_a$–$C_m$ bond length ranges in Ni(TMP) (1.375 (2)–1.380 (2) Å), Ni(TMC) (1.367 (2)–1.401 (2) Å), and Ni(TMiBC) (1.313 (6)–1.435 (6) Å).

A striking feature of both the Ni(TMP) and Ni(TMC) crystal structures is a good internal consistency between chemically equivalent[25b,43] bond lengths within the macrocycle. On the basis

---

(39) In the text $C_a$ refers to the $\alpha$-pyrrole or $\alpha$-pyrroline carbon atoms, $C_b$ refers to the $\beta$-pyrrole or $\beta$-pyrroline carbon atoms, $C_m$ refers to the meso carbon atoms, and $C_{Me}$ refers to the methyl carbon atoms. Hoard, J. L. *Ann. N.Y. Acad. Sci.* **1973**, *206*, 18–31.

(40) The $C_b$–$C_b$ bonds of porphyrins and reduced porphyrins can be readily affected by modeling and experimental errors. Librational motion can cause bond foreshortening that for porphyrin-type molecules would be most apparent in the $C_b$–$C_b$ bond lengths. Perhaps more importantly, the derived positional and thermal parameters can be biased if the aspherical valence electron density of an atom is significantly unsymmetrical. This was demonstrated recently for Ni(TMP), where the average $C_b$–$C_b$ bond length derived from an aspherical model refinement was 0.02 Å longer than that derived from a conventional spherical model refinement (ref 25c).

(41) Spaulding, L. D.; Andrews, L. C.; Williams, G. J. B. *J. Am. Chem. Soc.* **1977**, *99*, 6918–6923.

(42) Strauss, S. H.; Silver, M. E.; Ibers, J. A. *J. Am. Chem. Soc.* **1983**, *105*, 4108–4109.

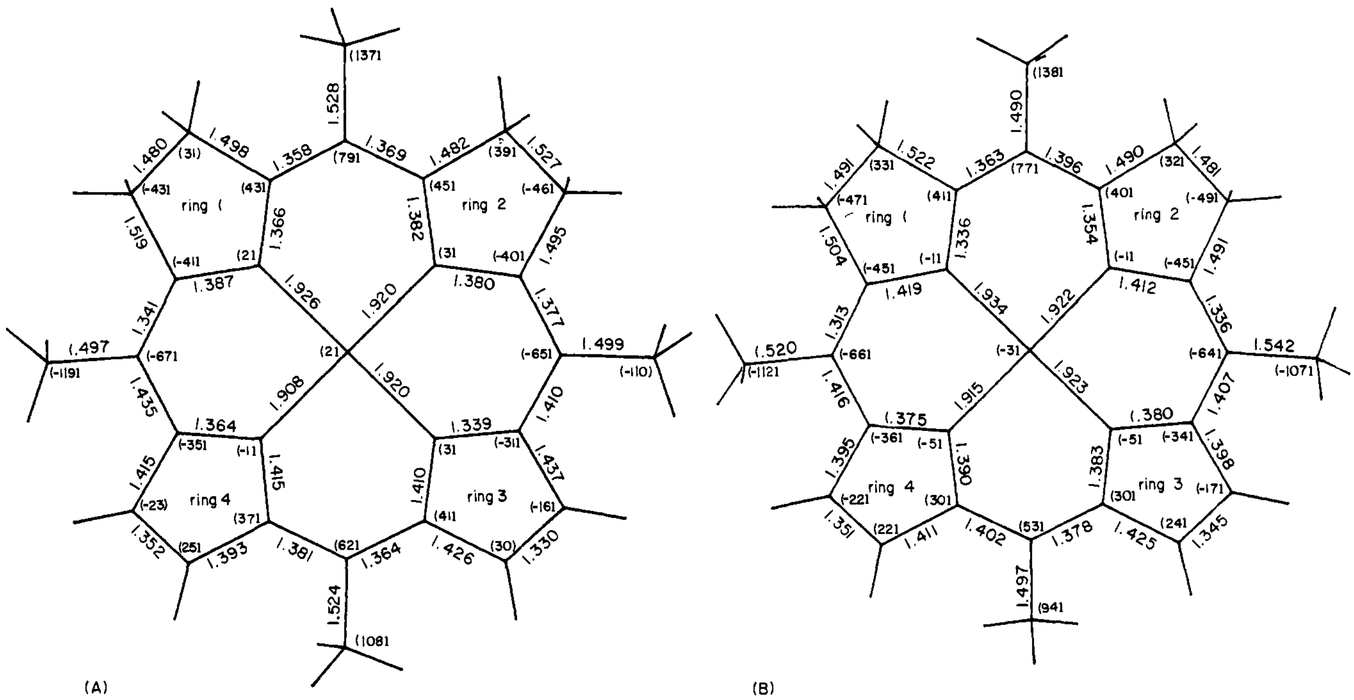

**Figure 3.** Selected bond distances (Å) and deviations (Å × $10^3$; $\sigma \approx 0.003–0.006$ Å) from the plane of the 24-atom macrocyclic skeleton for the two independent molecules of Ni(TMiBC). Estimated standard deviations (Å) for bond lengths in Ni(TMiBC) are as follows: Ni–N, 0.003; N–$C_a$, 0.005–0.006; $C_a$–$C_b$, 0.005–0.006; $C_a$–$C_m$, 0.005–0.007; $C_b$–$C_b$, 0.006–0.008; $C_m$–$C_{Me}$, 0.005–0.006.

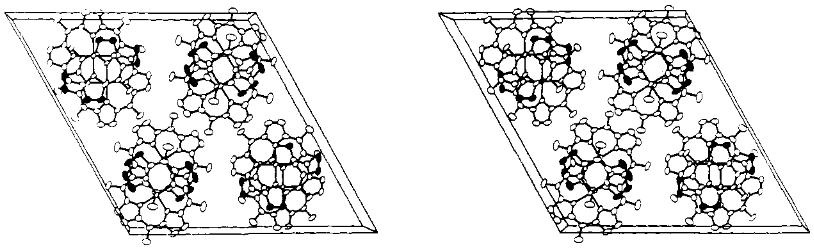

**Figure 4.** Stereoscopic diagram of the packing for Ni(TMiBC) viewed down the *b* axis (50% probability thermal ellipsoids). Hydrogen atoms have been omitted, and the pyrroline β-carbon atoms have been shaded for clarity.

of chemical equivalence alone, Ni(TMiBC) should possess a pseudo-mirror plane perpendicular to the plane of the macrocycle and including atoms C(5), Ni, and C(15). A careful examination of Figure 3 shows that this is not the case for Ni(TMiBC); bond lengths related by this noncrystallographic symmetry element are clearly not equal (i.e., C(4)′–C(5)′ = 1.363 (6) Å and C(5)′–C(6)′ = 1.396 (6) Å). In addition, the overall bond length patterns for the two independent molecules are quite different. This structural discrepancy led to a more thorough analysis of the molecular packing in the crystal structure. What is found, as illustrated in Figures 4 and 5, is that the two independent molecules have different packing environments.[43b] With respect to atom overlap between neighboring molecules, molecule 1 can be said to have an asymmetric packing mode (Figure 5A) and molecule 2 can be said to have a symmetric packing mode (Figure 5B). Intramolecular distortions arising from close intermolecular contacts have been previously documented for metallophthalocyanines[44] and for the Ni–N bonds in Ni(TMP).[25c] We therefore expect that the overall bonding patterns of the two independent molecules of Ni(TMiBC) should be affected by the differences in packing environment, but the effect is not significant.

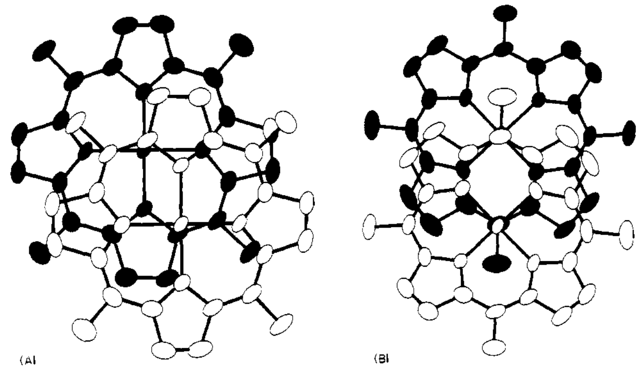

**Figure 5.** Projected views of the two independent Ni(TMiBC) molecules illustrating the different packing modes: (A) asymmetric packing mode, molecule 1; (B) symmetric packing mode, molecule 2.

The overall conformation of a metalloporphyrin or reduced metalloporphyrin is a function of many factors: the size of the metal ion, the magnitude of the delocalization energy, the number of pyrroline rings, packing energy, etc. Unstrained free-base porphyrins and reduced porphyrins have a strong tendency to be

---

[43] (a) Ni(TMP) is a planar molecule with fourfold chemical symmetry. Ni(TMC) has an $S_4$ ruffled conformation with a noncrystallographic twofold axis passing through the pyrroline ring and the opposite pyrrole ring. All chemically equivalent bond lengths within the two macrocycles agree to better than three standard deviations. The significant difference in the Ni–N bond lengths in Ni(TMP) may be related to intermolecular interactions (ref 25c). (b) The difference in packing modes for the two independent molecules of Ni(TMiBC) allows one to speculate on the nature of the low-temperature phase change described in the experimental section. The shortest non-hydrogen intermolecular contacts between slipped-stack neighbors is 3.38 Å for molecule 1 and 3.58 Å for molecule 2. The difference might become crucial as the unit cell contracts upon cooling, i.e., the slipped-stack neighbors of molecule 1, because of their inherently closer contacts, might be forced to shift in such a way as to destroy the *c*-glide symmetry.

[44] Mason, R.; Williams, G. A.; Fielding, P. E. *J. Chem. Soc., Dalton Trans.* **1978**, 676–683.

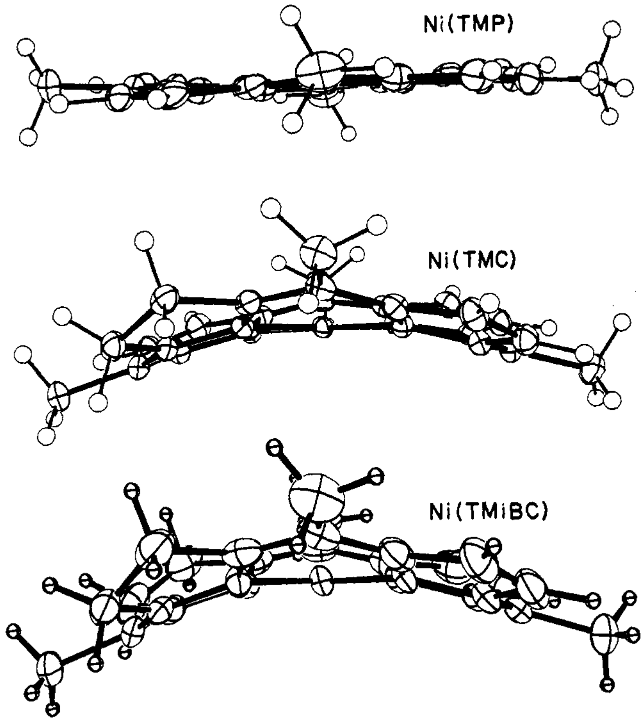

**Figure 6.** Views of Ni(TMP), Ni(TMC), and Ni(TMiBC) along the N(2)–Ni–N(3) planes. The non-hydrogen atoms are drawn at the 50% probability level while the hydrogen atoms are drawn on an arbitrary scale.

**Table X.** A Comparison of Average Bond Lengths (Å) and Angles (deg) for Ni(TMP), Ni(TMC), and Ni(TMiBC)

| | Ni(TMP) | Ni(TMC) | Ni(TMiBC) |
|---|---|---|---|
| Ni–N | 1.953 (14)[b] | 1.922 (6) | 1.916 (7) |
| Ni–N*[a] | | 1.936 (1) | 1.926 (6) |
| N–$C_a$ | 1.384 (3) | 1.384 (12) | 1.382 (24) |
| N*–$C_a$* | | 1.376 (2) | 1.378 (28) |
| $C_a$–$C_m$ | 1.378 (2) | 1.392 (10) | 1.397 (23) |
| $C_a$*–$C_m$ | | 1.368 (2) | 1.355 (26) |
| $C_a$–$C_b$ | 1.439 (3) | 1.432 (4) | 1.412 (16) |
| $C_a$*–$C_b$* | | 1.506 (2) | 1.499 (14) |
| $C_b$–$C_b$ | 1.334 (5) | 1.355 (6) | 1.343 (10) |
| $C_b$*–$C_b$* | | 1.516 (2) | 1.497 (22) |
| $C_a$–N–$C_a$ | 104.8 (4) | 105.4 (3) | 105.6 (10) |
| $C_a$*–N*–$C_a$* | | 107.8 (1) | 108.3 (9) |
| N–$C_a$–$C_m$ | 126.3 (3) | 125.5 (3) | 124.8 (8) |
| N*–$C_a$*–$C_m$ | | 126.2 (1) | 125.7 (12) |
| N–$C_a$–$C_b$ | 110.2 (2) | 110.1 (3) | 109.3 (10) |
| N*–$C_a$*–$C_b$* | | 112.0 (1) | 110.7 (14) |
| $C_b$–$C_a$–$C_m$ | 123.5 (4) | 124.1 (3) | 125.3 (13) |
| $C_b$*–$C_a$*–$C_m$ | | 121.7 (1) | 123.0 (20) |
| $C_a$–$C_m$–$C_a$ | 121.9 (1) | 120.9 (1) | 122.2 (13) |
| $C_a$–$C_m$–$C_a$* | | 120.9 (1) | 121.8 (17) |
| $C_a$*–$C_m$–$C_a$* | | | 119.9 (17) |
| $C_a$–$C_b$–$C_b$ | 107.4 (1) | 107.2 (2) | 107.7 (14) |
| $C_a$*–$C_b$*–$C_b$* | | 103.0 (1) | 103.5 (9) |

[a] An asterisk denotes an atom associated with a pyrroline ring. [b] An estimated standard deviation in parentheses is the larger of that estimated for a single observation from the inverse matrix or from the values averaged.

planar in the crystalline state;[18-20,45] such a conformation is favorable for maximum $\pi$ delocalization. Complexation of a metal atom with a porphyrin or reduced porphyrin raises the possibility of a discrepancy between the optimum M–N separation and the core size of the planar macrocycle. An M–N distance can be shortened by an $S_4$ ruffling of the molecule, while a doming distortion can lead to a lengthening of the M–N bond length. Therefore the maintenance of a planar molecule is in direct conflict with the optimization of the M–N bond length when there is a difference between the core size and the ion size. As an example, a normal Ni–N bond length for a square-planar monodentate system is 1.85 Å.[46] The existence of two crystalline forms of Ni(OEP), one of which is planar with an average Ni–N distance of 1.958 (2) Å[47] and the other of which is significantly distorted with an average Ni–N distance of 1.929 (3) Å,[48] is usually taken as evidence that the balance between the two forces is rather delicate.[49] However, most metalloporphyrins are relatively planar,[45] and it can therefore be concluded that maintenance of planarity is the more important factor in the determination of the conformation for a porphyrin.

For reduced porphyrins two of the conformational factors are changed relative to the corresponding metalloporphyrin. The introduction of a pyrroline ring (or rings) into the macrocycle leads to a decrease in the delocalization energy owing to a disruption of the $\pi$-bonding system. Second, a reduced porphyrin has an intrinsically larger core size,[42,49] thus potentially increasing the M–N separation. Both of these factors are favorable for a distortion of the molecule when a difference in core size and ion size exists. It is therefore not surprising that for reduced metalloporphyrins where the metal ion has an optimum M–N distance <1.99 Å, a significant conformational distortion occurs. This has recently been illustrated in two molecular series (Fe(OEP)[50] and Fe(OEC)[42]; Ni(OEP)[47,48] and Ni(OEiBC)[18]) where the reduced metalloporphyrins are more distorted than the corresponding porphyrins. As illustrated in Figure 6, Ni(TMiBC) and Ni(TMC) both have conformations significantly more distorted than Ni(TMP). Correspondingly, the Ni–N distances are shorter for the reduced molecules (Table X).

Traditionally, conformational analysis of a porphyrin or reduced porphyrin follows from a qualitative investigation of the magnitude and sign of the atomic deviations from the 24-atom macrocycle best plane. From the pattern of these deviations the molecule is described as "planar", "ruffled", or "domed".[51] Dihedral angles ($\theta$) between the pyrrole and/or pyrroline rings are often reported as a quantitative measure of a particular distortion. An analysis of the pattern of atomic deviations in Figure 3 shows that both independent molecules of Ni(TMiBC) possess an $S_4$-ruffled conformation with maximum deviations from the planes of 0.788 (4) and 0.766 (5) Å and average deviations of 0.35 and 0.34 Å. The $\theta$ angles between opposite pyrrole and pyrroline rings range from 42° to 45° with an average $\theta$ value of 43° for Ni(TMiBC). This indicates a greater degree of distortion relative to a crystallographically rigorous $\theta$ value of 0° for Ni(TMP) and a mean $\theta$ value of 37° for Ni(TMC). By comparison the two isomers of Ni(OEiBC)[18] have an average $\theta$ value of 48°.

Unless a molecule possesses crystallographic site symmetry (for example, $\bar{4}$ site symmetry for the $S_4$-ruffled Fe(TPP)[24,52]), the dihedral angles between opposite rings are not necessarily a rigorous measure of the magnitude of a particular distortion. The overall dihedral angle can actually be a convolution of many factors, such as the deviation of a pyrroline ring from planarity or distortions owing to packing effects. Its use as a quantitative measure of distortion is thus somewhat ambiguous. Another shortcoming in this type of conformational analysis is that no knowledge is gained about how the distortion is actually relieved throughout the macrocycle. Additional information concerning the mode of molecular distortion can be obtained by calculating the atomic pyramidalization and bond twist angles from the

---

(45) A compilation of stereochemical parameters for free base and metalloporphyrins can be found in Jameson et al.: Jameson, G. B.; Robinson, W. T.; Ibers, J. A. "Hemoglobin and Oxygen Binding", Ho, C., Ed.; Elsevier-North Holland, Inc.: Amsterdam, 1982; pp 25–35.

(46) Sacconi, L. *Transition Met. Chem.* (*N.Y.*) **1968**, *4*, 199–298.

(47) Cullen, D. L.; Meyer, E. F., Jr. *J. Am. Chem. Soc.* **1974**, *96*, 2095–2102.

(48) Meyer, E. F. Jr. *Acta Crystallogr., Sect B* **1972**, *B28*, 2162–2167.

(49) Hoard, J. L. *Ann. N.Y. Acad. Sci.* **1973**, *206*, 18–31.

(50) The X-ray structure of Fe(OEP) has recently been determined in this laboratory: Strauss, S. H.; Silver, M. E.; Ibers, J. A., manuscript in preparation.

(51) Murray-Rust, P.; Kratky, C. *Int. Congr. Crystallogr. Abstr., 12th* **1981**, *04.1–07*, C82.

(52) Collman, J. P.; Hoard, J. L.; Kim, N.; Lang, G.; Reed, C. A. *J. Am. Chem. Soc.* **1975**, *97*, 2676–2681.

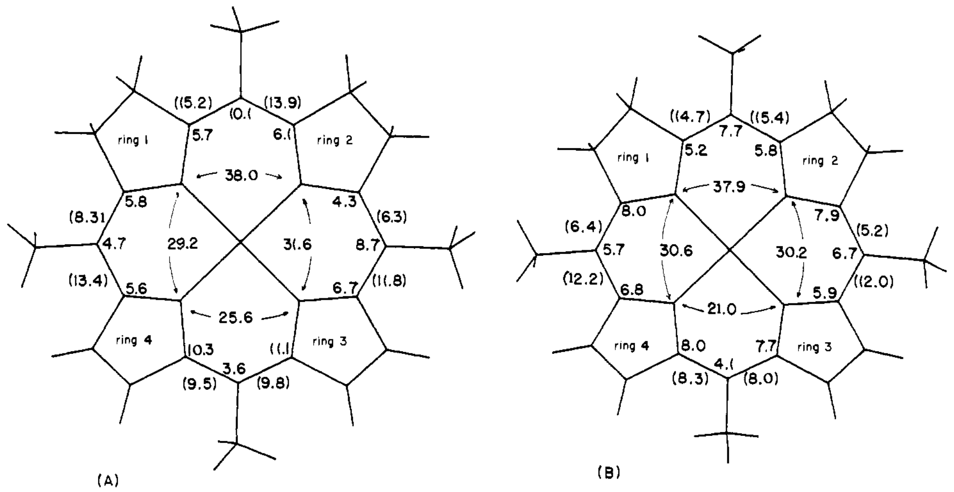

**Figure 7.** Conformational parameters (in degrees) for the two independent molecules of Ni(TMiBC). Pyramidalization angles ($\chi$) are adjacent to the $C_a$ and $C_m$ atoms. Twist angles ($\tau$) are given in parentheses next to the $C_a$–$C_m$ bonds. Dihedral angles ($\theta$) between adjacent rings are situated between the arrows.

**Table XI.** Conformational Comparison of Ni(TMP), Ni(TMC), and Ni(TMiBC)

| | Ni(TMP)[a] | Ni(TMC)[a] | Ni(TMiBC)[b] |
|---|---|---|---|
| 24-atom best plane | | | |
| mean dev, Å | 0.05 | 0.29 | 0.35[c] |
| max dev, Å | 0.12 | 0.60 | 0.78 |
| dihedral angle ($\theta$),[d] deg | 0 | 37 | 43 |
| mean $\chi_{C_a}$, deg | 2.7 (0.9–3.8)[e] | 6.2 (4.0–10.5) | 7.0 (4.3–11.1) |
| mean $\chi_{C_m}$, deg | 0.6 (0.5–0.8)[e] | 6.0 (5.6–6.5) | 6.4 (3.6–10.1) |
| mean $\tau_{C_a-C_m}$, deg | 4.8 (2.0–7.3)[e] | 9.9 (6.7–13.4) | 10.7 (5.2–15.4) |

[a] Reference 25b. [b] This work. [c] Ni(TMiBC) parameters are averaged for the two independent molecules. [d] Dihedral angle between opposite pyrrole or pyrroline rings. [e] $\chi(C_a)$, $\chi(C_m)$, and $\tau_{C_a-C_m}$ are expressed in terms of torsion angles $\omega$: $\chi(C_a) = \omega(C_bC_aC_mC_{Me}) - \omega(NC_aC_mC_{Me}) + \pi(\text{modulo } 2\pi)$; $\chi(C_m) = \omega(C_aC_mC_aN) - \omega(C_{Me}C_mC_aN) + \pi(\text{modulo } 2\pi)$; $\tau_{C_a-C_m} = [\omega(C_bC_aC_mC_{Me}) + \omega(NC_aC_mC_a)]/2$. Reference 53. Me = methyl carbon.

formalism of Dunitz[53] as originally applied to secondary amide linkages[54] and more recently to bipyridine ligands.[55] In this way one can identify the specific combination of out-of-plane bending distortion and twisting distortion that constitutes the overall conformation of a macrocycle.

Pyramidalization ($\chi$) and twist angles ($\tau$), which are out-of-plane bending coordinates and intraligand twisting coordinates, respectively, have been calculated for the $C_a$ atoms, $C_m$ atoms, and the $C_a$–$C_m$ bonds and are projected on the molecular skeletons in Figure 7. The $\chi(C_a)$ and $\chi(C_m)$ values are measures of the pyramidalization of the $C_a$ and $C_m$ atoms, and $\tau$ is a measure of the twist about the C–C bonds. If no pyramidalization occurs for adjacent $C_a$ and $C_m$ atoms ($\chi(C_a) = \chi(C_m) = 0.0$), then the angle $\tau$ is equal to the dihedral angle between the two planes defined by N, $C_a$, $C_b$ and $C_{Me}$, $C_m$, $C_a$; if an atom has tetrahedral pyramidalization then $\chi = 60°$ for that atom. For comparison, the dihedral ($\theta$) angles between adjacent pyrrole (and/or pyrroline) rings are also displayed. This type of conformational analysis is useful for two reasons. (i) A more informative overall description is obtained. An analysis based solely on the atomic deviations from the 24-atom macrocycle plane would lead one to believe that there is no significant difference between the conformations of the two independent molecules—maximum deviations of 0.788 (4) and 0.766 (5) Å, respectively, and average deviations of 0.35 and 0.34 Å, respectively. However, the conformational differences between molecules 1 and 2 are reflected in the ranges of pyramidalization parameters ($\chi$) (Table XI); molecule 1 is found to have a wider range of pyramidalization angles compared with the more even distribution in molecule 2. This is presumably related to differences in packing requirements. (ii) Specific modes of distortion can be more easily identified. For example, the $\theta$ angles between adjacent pyrroline rings are twice as large as the $\theta$ angles between adjacent pyrrole rings. In both molecules this can be seen to arise from $C_a$–$C_m$ twist distortions ($\tau$) between the pyrroline rings that are roughly twice as large as those between the pyrrole rings.

Overall, if one compares the Ni(TMiBC) $\chi$ and $\tau$ values with those calculated for Ni(TMP) and Ni(TMC) (Table XI), one identifies a significant increase in conformational distortion going from the porphyrin to the chlorin, but only a slight increase in going from the chlorin to the isobacteriochlorin. This implies that the additional strain is evenly distributed throughout the two Ni(TMiBC) molecules.

**Acknowledgment.** This work was kindly supported by the National Institutes of Health (HL 13157). In addition, M.P.S. thanks the Korea Science and Engineering Foundation for financial assistance.

**Registry No.** Ni(TMiBC), 91054-04-5; $CH_3CH(OC_2H_5)_2$, 105-57-7; pyrrole, 109-97-7; TM porphyrinogen, 91054-05-6.

**Supplementary Material Available:** Anisotropic thermal parameters (Table V), hydrogen atom parameters (Table VI), and the final values of $10|F_o|$ and $10|F_c|$ are available (20 pages). Ordering information is given on any current masthead page.

---

[53] Dunitz, J. D. "X-ray Analysis and the Structure of Organic Molecules"; Cornell University Press: Ithaca, NY, 1979; Chapter 7, pp 328–337.

[54] Winkler, F. K.; Dunitz, J. D. *J. Mol. Biol.* **1971**, *5*, 169–177.

[55] Cordes, A. W.; Durham, B.; Swepston, P. N.; Pennington, W. T.; Condren, S. M.; Jensen, R.; Walsh, J. L. *J. Coord. Chem.* **1982**, *11*, 251–260.